TOPICAL REVIEW — 2D materials: physics and device applications

Optical properties of phosphorene

Jiong Yang and Yuerui Lu(卢曰瑞)†

Research School of Engineering, College of Engineering and Computer Science, the Australian National University, Canberra ACT 2601, *Australia*

(Received 12 September 2016; published online 18 January 2017)

Phosphorene is a two-dimensional semiconductor with layers-dependent bandgap in the near-infrared range and it has attracted a great deal of attention due to its high anisotropy and carrier mobility. The highly anisotropic nature of phosphorene has been demonstrated through Raman and polarization photoluminescence measurements. Photoluminescence spectroscopy has also revealed the layers-dependent bandgap of phosphorene. Furthermore, due to the reduced dimensionality and screening in phosphorene, excitons and trions can stably exist at elevated temperatures and have large binding energies. The exciton and trion dynamics are thus detected by applying electrical bias or optical injection to the phosphorene system. Finally, various optical and optoelectronic applications based on phosphorene have been demonstrated and discussed.

Keywords: two-dimensional material, phosphorene, exciton, anisotropy

PACS: 42.25.Ja, 42.50.Ct, 68.35.bg **DOI:** 10.1088/1674-1056/26/3/034201

1. Introduction

Since the rise of graphene[1,2] two-dimensional (2D) materials, including transition metal dichalcogenides (TMDs), hexagonal boron nitride (hBN), and phosphorene, have attracted a great deal of attention.[3–11] In the family of 2D materials, phosphorene is a relatively new member and it has shown unique optical and optoelectronic properties, due to its highly anisotropic nature originating from its puckered structure.[12–14] Moreover, phosphorene differs from other 2D materials in that it always possesses a direct bandgap, from monolayer to bulk form,[12,15] while in contrast, graphene, being a semimetal and TMD, exhibits a direct bandgap only when thinned down to monolayer.[2,16–18] The direct bandgap of phosphorene does vary with the number of layers, from ~ 2 eV for monolayer phosphorene all the way down to ~ 0.3 eV for bulk black phosphorus.[15,19–21] Similar to other 2D materials, few-layer phosphorene was first characterized on its transport properties by measuring transistor performance.[22–25] The anisotropic and layers-dependent charge transfer in few-layer phosphorene-gold hybrid systems has been experimentally demonstrated, and it will benefit future designers of electronic and optoelectronic heterostructure devices with phosphorene.[26] Characterization of the optical properties of phosphorene, including Raman scattering and photoluminescence (PL) spectroscopy, is essential to further understand its electronic band structure, crystalline orientation, and highly anisotropic exciton/trion dynamics. An exciton is a quasi-particle formed by one electron and one hole through Coulombic interaction, and a trion is a charged exciton consisting of two electrons and one hole (or two holes and one electron).[27] Due to the reduced dimensionality and screening in the highly anisotropic phosphorene layer, excitons and trions formed in a 2D phosphorene platform exhibit quasi-one-dimensional (quasi-1D) performance and possess binding energies that are much larger than those in quasi-2D quantum wells and other isotropic 2D materials, such as TMDs.[17,18,27–30] All the above-mentioned unique optical properties of few-layer phosphorene have been systematically characterized in experiments and theoretically explained.

In this paper, we discuss the optical properties of phosphorene and its potential applications, based on our recent progress as well as publications from other groups. We start from the Raman and PL spectroscopy of few-layer phosphorene to understand its anisotropic crystal structure and layers-dependent bandgap. Then, we discuss the exciton and trion dynamics, especially the anisotropic, quasi-1D trion in few-layer phosphorene. We also discuss the surface defect-induced exciton brightening and strong PL emission in monolayer phosphorene. Finally, we discuss the future prospects of 2D phosphorene in numerous applications.

2. Raman and PL characterization

Since the rediscovery of black phosphorus as a 2D material, called phosphorene, it has been predicted with extraordinary anisotropy with its puckered crystal structure.[4,12] Figure 1(a) displays the puckered structure of phosphorene. Raman spectroscopy is a powerful tool to characterize the electronic and structural properties of few-layer phosphorene. By measuring the polarized Raman spectra of a 15-layer (15 L) phosphorene (Fig. 1(b)), we successfully obtained the angle-dependent Raman intensities of different Raman vibrational modes, as shown in Fig. 1(c). It can be seen that A_g^2 and B_{2g}

†Corresponding author. E-mail: yuerui.lu@anu.edu.au

© 2017 Chinese Physical Society and IOP Publishing Ltd

modes show similar strong polarization dependence but opposite trends. This is because they are both in-plane vibrations and perpendicular to each other. The crystalline orientation of the 15 L phosphorene sample was then quickly determined based on the polarization-dependent Raman measurements, as indicated in Fig. 1(d). Thus polarized Raman spectroscopy provides a non-destructive, accurate method to determine the crystalline orientation of phosphorene, due to its high anisotropy, which can be generalized to other highly anisotropic platforms. Similar to TMDs, few-layer phosphorene's Raman modes vibrational frequencies are layers-dependent and can be utilized to determine the number of layers.[31] Besides, when phosphorene samples are well protected from oxidation, the sample thickness will be proportional to the ratio between A_g^1 mode, the out-of-plane vibration mode, and Raman peak of the Si substrate.[32] Besides, phase-shifting interferometry (PSI) has been proved to be another very fast, accurate, and non-destructive approach to determine the layer number of 2D materials, especially for fast-degrading materials such as graphene.[6,20,26,33] Considering the fact that few-layer phosphorene is easily oxidized and unstable,[20,31] these optical methods to count the layers of few-layer phosphorene samples can be very useful for research and future applications.

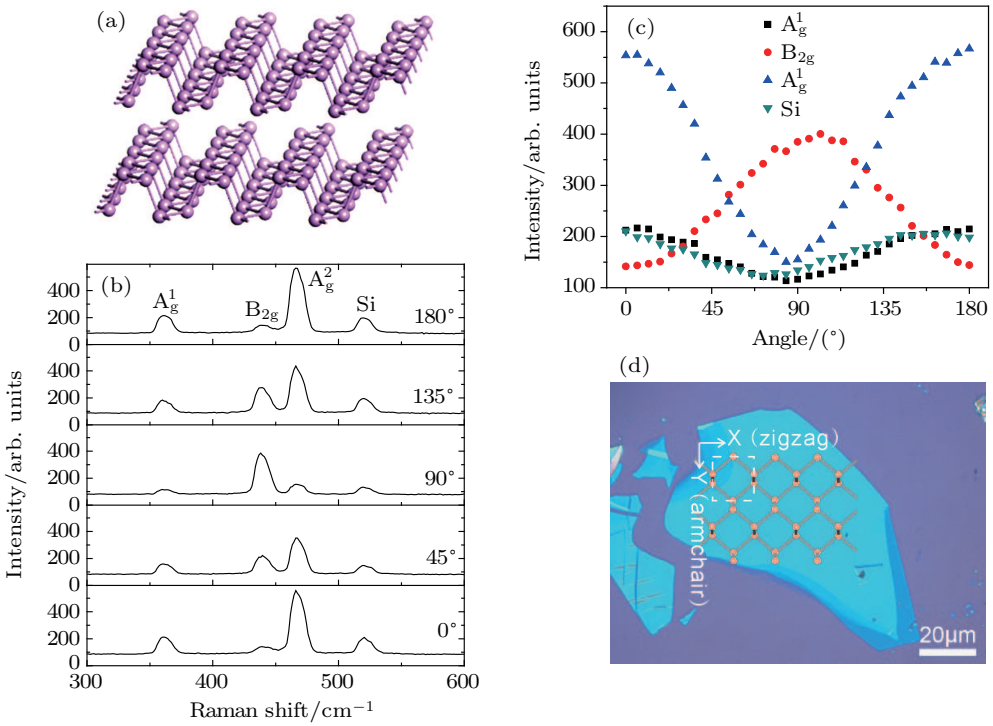


Fig. 1. (color online) Raman characterization of phosphorene. (a) Crystal structure of phosphorene. (b) Polarized Raman spectra of a 15 L phosphorene sample. (c) Angle-dependent Raman mode intensity extracted from the spectra in panel (b). (d) Crystalline orientation of the 15 L phosphorene sample. Figure reproduced from Refs. [15] and [20].

PL spectroscopy is another commonly used method for semiconductor characterization, used to detect band structure information. We conducted PL measurements on 1 L to 5 L phosphorene samples and the PL emission peaks are distinctly located from the visible to near infrared range. Figure 2(a) displays the normalized layers-dependent PL spectra for 1–5 L phosphorene samples. The measured PL peaks are attributed to the emission from exciton recombination, which represents the lower bounds of the electrical bandgap for few-layer phosphorene. It is clear that phosphorene samples with different numbers of layers have different PL emission wavelengths. Once, there was a huge controversy on the layer number identification of very-few-layer (1 L or 2 L) phosphorene due to its fast degradation.[14,31,32] Since our systematic investigation on the layers-dependent PL of phosphorene samples, more experiments have been carried out, confirming that the PL emission of monolayer phosphorene is around 700 nm.[21,34] By extracting the PL emission energy from Fig. 2(a), we have drawn the peak energy for 1–5 L phosphorene samples in Fig. 2(b). The peak energies of the phosphorene samples decrease rapidly with the increase of layer count, due to the quantum confinement effect. By fitting the peak energy vs. layer count data, the optical gap of bulk black phosphorus is estimated to be abound 0.3 eV, which is consistent with the measured energy gap of black phosphorus.[4,35] As shown by the error bar in Fig. 2(b), we measured several samples for each layer count, and the PL peak locations are constant among the samples of the same layer count, as indicated in Table 1. This systematic investigation of layers-dependent PL on phosphorene confirms theoretical predictions and provides sufficient information for

future optoelectronic applications.

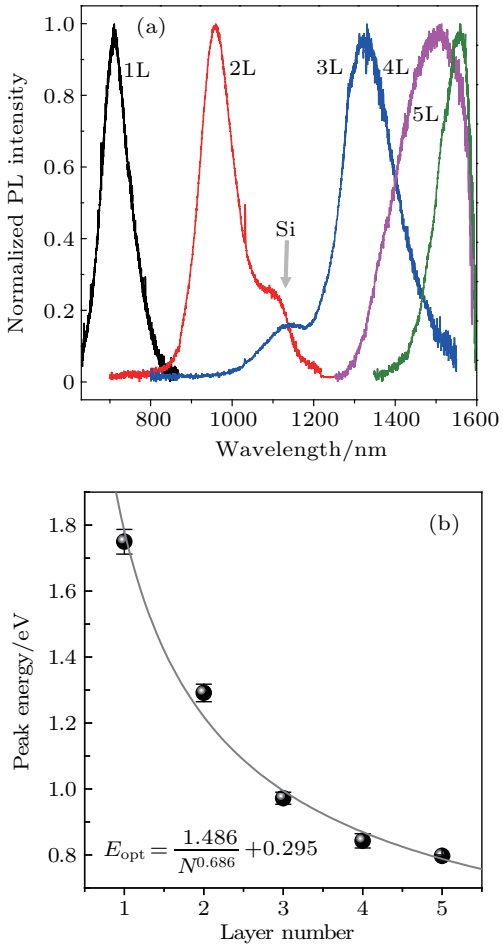


Fig. 2. (color online) PL characterization of 1–5 L phosphorene samples. (a) Normallized PL spectra of the samples. (b) PL peak energy for the samples. Figure reproduced from Ref. [20].

Table 1. PL peak locations for phosphorene samples with different layer counts.

Sample	Layer count	PL peak wavelength/nm	PL peak energy/eV
Sample-1	1L	701	1.77
Sample-2	1L	705	1.76
Sample-3	1L	702	1.77
Sample-4	2L	961	1.29
Sample-5	2L	965	1.29
Sample-6	3L	1268	0.98
Sample-7	3L	1264	0.98
Sample-8	4L	1413	0.88
Sample-9	4L	1441	0.86
Sample-10	5L	1558	0.80
Sample-11	5L	1555	0.80
Sample-12	5L	1557	0.80

3. Exciton and trion dynamics

Trion binding energy in quasi-2D quantum wells is in the range of 1–5 meV, and trions in such a quasi-2D system are very unstable and can only exist at cryogenic temperatures.[27,29] When the dimensionality is reduced to real 2D, i.e., monolayer of TMD materials, the measured trion binding energy is up to 20–30 meV.[17,18,30,36,37] With a further decrease of platform dimensionality and screening, trions in 1D space such as carbon nanotubes have exhibited remarkably high binding energies in the range of 100–200 meV. Excitons and trions inside few-layer phosphorene are confined in a quasi-1D space due to the highly anisotropic nature of phosphorene; thus we can imagine that trions in few-layer phosphorene can exist stably at elevated temperature and have a comparatively large binding energy.

We have experimentally demonstrated the quasi-1D nature of excitons and trions in a 3 L phosphorene sample by both excitation and emission polarization PL measurements. Figure 3(a) is a schematic of our experimental setup. The excitation source is tuned to be linearly polarized by a half-wave plate and the emission polarization will be detected by a polarizer. For excitation polarization measurements, the polarizer on the emission side will be taken away and the half-wave plate on the excitation side will be rotated to change θ_1. For emission polarization measurements, the half-wave plate on the excitation side will be rotated to the angle where the maximal PL intensity can be achieved, and the polarizer on the emission side will be rotated to change θ_2. From our experimental results, the trion emission of a 3 L phosphorene sample shows a very strong polarization dependence, as shown in Fig. 3(b), indicating that the absorption of excitation source by the 3 L phosphorene sample is highly anisotropic. Both exciton and trion peaks of the same sample show significant emission polarization, as indicated in Figs. 3(c) and 3(d). Such PL excitation and emission polarization dependence in phosphorene verifies its anisotropic nature. Tran *et al.* and Qiao *et al.* have previously calculated and pointed out the anisotropic nature of excitons and trions in phosphorene,[12,38] and Wang *et al.* and Xia *et al.* have also demonstrated the anisotropic PL emission and infrared spectroscopy, respectively, for few-layer phosphorene.[13,14] All these experimental findings provide useful information for future optoelectronic applications based on few-layer phoshorene.

By fitting the gate-dependent PL spectra from the 3 L phosphorene sample shown in Fig. 3(e), two distinct peaks show up and are attributed to exciton and trion emissions. Exciton and trion peaks can be tuned by an external bias, due to extra carrier injection. The trion binding energy is extracted to be $\sim$ 160 meV. This value is comparable with that measured in carbon nanotubes, further confirming that the excitons and trions are confined in a quasi-1D space in phosphorene due to its strong anisotropic nature. By making use of the highly anisotropic excitons and trions, large and uniform few-layer phosphorene can act like an array of carbon nanotubes for real optoelectronic applications.

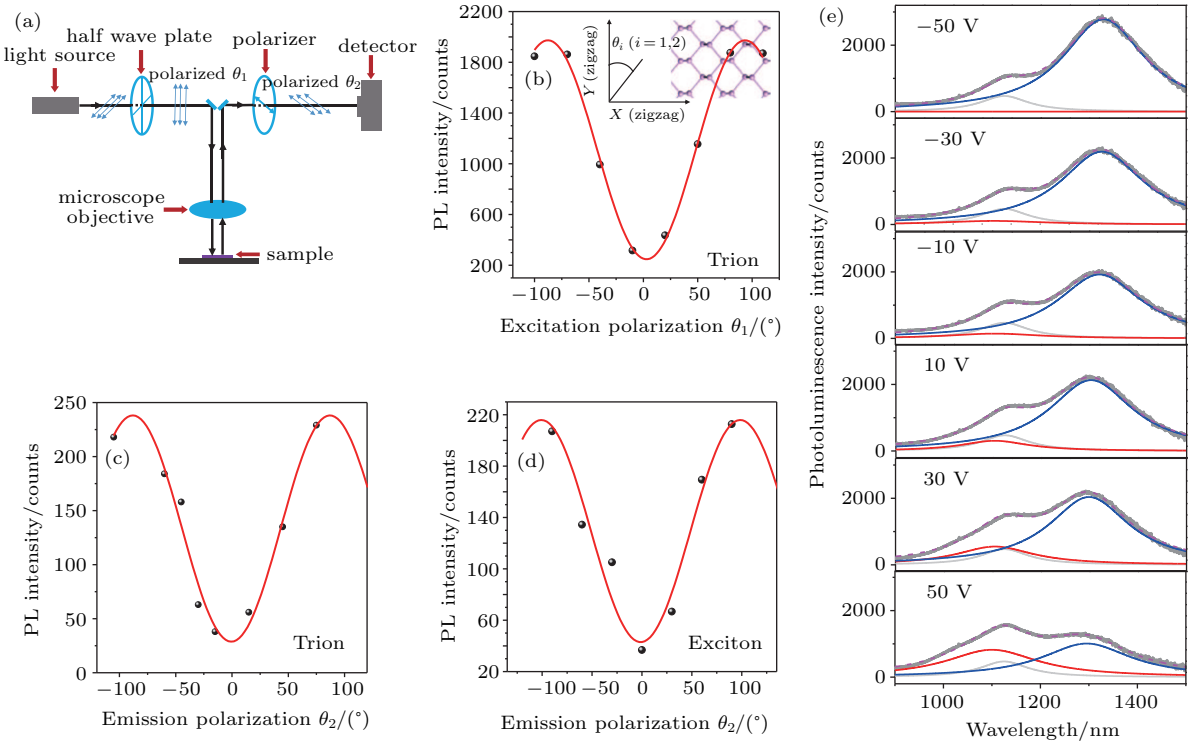


Fig. 3. (color online) Excitation and emission polarization PL measurements of a 3 L phosphorene sample. (a) Schematic plot of the experimental setup. (b) Excitation polarization of the trion peak. (c) Emission polarization of the trion peak. (d) Emission polarization of the exciton peak. (e) Gate-dependent PL measurements. Figure reproduced from Ref. [28].

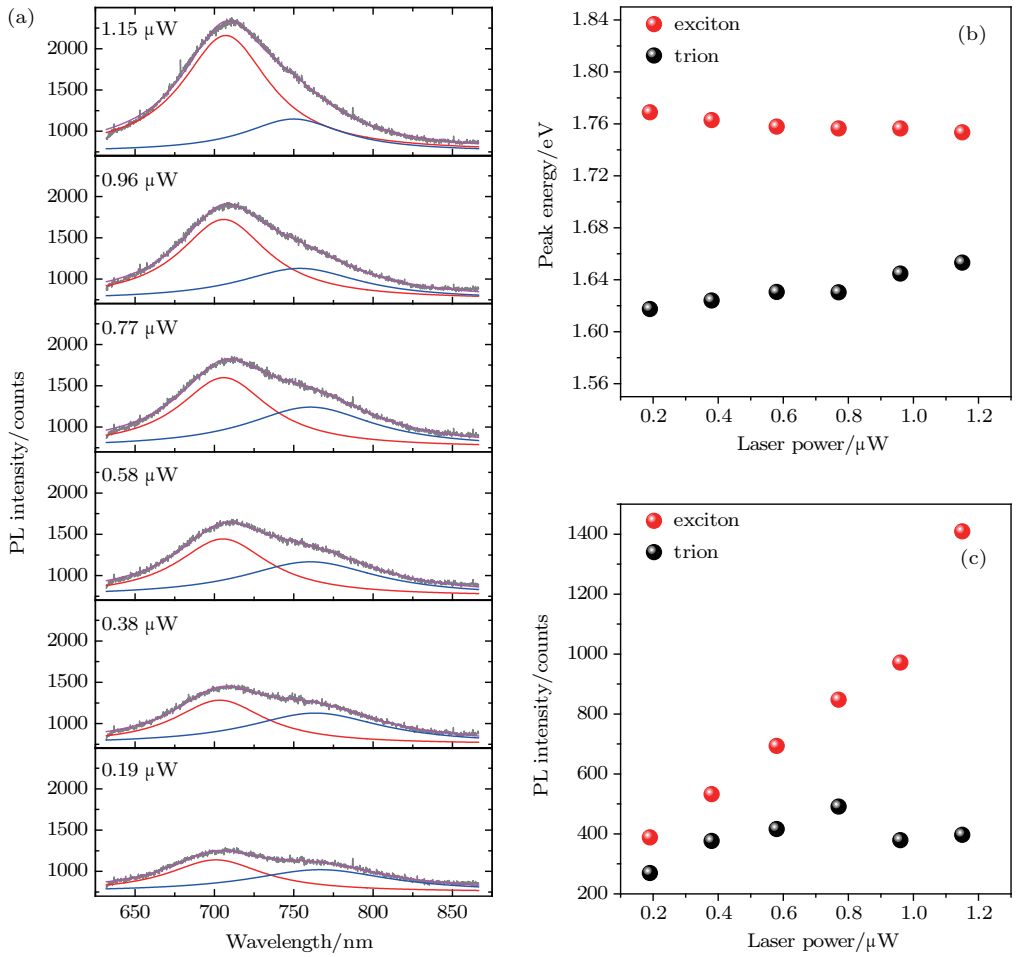


Fig. 4. (color online) Exciton and trion dynamics under optical injection. (a) PL spectra under different excitation laser power. (b) Exciton and trion peak energies under different excitation laser power. (c) Exciton and trion peak intenstities under different excitation laser power. Figure reproduced from Ref. [20].

By applying an electric bias on a 3 L phosphorene sample, charge carriers are injected into the system, and the exciton and trion PL intensities are thus tuned. Direct optical injection is another yet simpler way to tune the exciton and trion dynamics in few-layer phosphorene. By increasing the excitation laser power, electron–hole pairs will be generated in the phosphorene system and excitons will be formed. Since the trion intensity will be limited by the initial doping, we should expect the trion peak intensity in PL measurements to saturate with increasing laser power. Figure 4 shows the exciton and trion dynamics in a monolayer phosphorene sample under direct optical injection. Each PL spectrum under different excitation laser power can be fitted into two peaks, which can be attributed to exciton and trion emissions. With an increase of laser power, the exciton peak gradually dominates the PL spectrum, indicating that more excitons have been formed by the injected electron–hole pairs, while the trion intensity reaches its maximum, limited by the sample's initial doping. The extracted trion binding energy for monolayer phosphorene is $\sim$ 100 meV (Fig. 4(b)), which is much larger than that measured in TMD materials. Note that the trion binding energy of 1 L phosphorene is smaller than that of the 3 L phosphorene sample. Normally, we would expect the opposite due to the quantum confinement effect. But here in very thin phosphorene samples, screening from the substrate has a huge impact on the trion binding energy. It is also clear that the trion intensity saturates with an increase of excitation laser power (Fig. 4(c)), consistent with our theoretical prediction.

4. Defect engineering

Phosphorene has attracted increasing attention among scientists because of its high anisotropy, direct bandgap, strong PL emission in the near-infrared range, excitons and trions confined in quasi-1D space, and large trion binding energy. However, few-layer phosphorene can easily be oxidized in the presence of light and moisture,[15,20,31,32,39–42] which greatly limits its future applications in the semiconductor industry. Several passivation methods have been proposed and successfully used to stabilize few-layer black phosphorus, such as coating Al_2O_3 with atomic layer deposition (ALD) and sandwiching phosphorene with hBN layers.[39,43–48]

We have demonstrated a new method to obtain few-layer phosphorene and to passivate it at the same time by combining O_2 plasma treatment and Al_2O_3 encapsulation. Figure 5 shows a schematic of the whole passivation process, and it can be seen that the phosphorene sample can be thinned down layer by layer before the Al_2O_3 encapsulation by precisely controlling the O_2 treatment conditions. By using this method, monolayer phosphorene samples protected by phosphorus oxide and

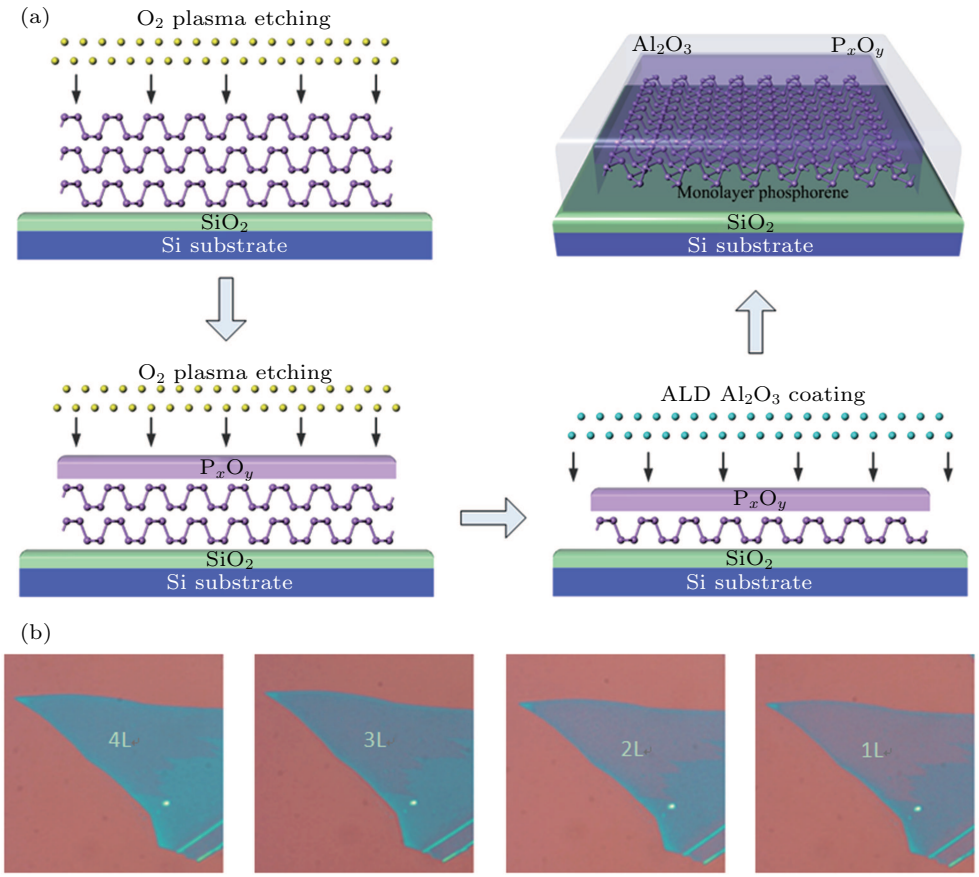


Fig. 5. (color online) Passivation of few-layer phosphorene by combining O_2 treatment and Al_2O_3 encapsulation. (a) Schematic plot of the whole passivation process. (b) Layer by layer thinning down of few-layer phosphorene with O_2 plasma. Figure reproduced from Ref. [33].

ALD Al_2O_3 layers can be used for more than two months without a significant decline in PL intensity. Furthermore, by controlling the O_2 plasma treatment process to over-etch the few-layer phosphorene sample, oxygen defects can be deliberately introduced, resulting in new sub-bands in the phosphorene band diagram and new PL emission lines. Among them, a new PL emission at $\sim$ 920 nm has been observed in experiments and is attributed to the bridge-type oxygen surface defects.[41]

Since phosphorene is a 2D material, the introduction of surface defects on phosphorene can also be achieved through substrate engineering. By using plasma-enhanced chemical vapor deposition (PECVD) on silicon oxide substrate, luminescent local states can be introduced in monolayer phosphorene. These luminescent local states can be considered to be a 0D light emission center, and thus will give much stronger light emission, similar to the conditions in 1D carbon nanotubes.[50] Figure 6(a) shows the schematic of free excitons being localized by surface defects on monolayer phosphorene and becoming localized 0D excitons. As shown in Fig. 6(b), much stronger PL emission is observed at $\sim$ 920 nm and is attributed to the carrier combination from the defects induced sub-bands. Polarization PL measurements (Figs. 6(c) and 6(d)) further reveal the anisotropic nature of the emission from those defect centers, so the defects can be considered to be surface point defects.

Recently, other work on oxidation of phosphorene has been published.[51–53] By designed and deliberate surface oxidation, the bandgap of phosphorene can be tuned. Besides, phosphorus oxide, the oxidation product of phosphorene, is also a semiconductor, and its bandgap can be tuned during the oxidation process. These all bring more possibilities for future applications of phosphorene and its oxides.

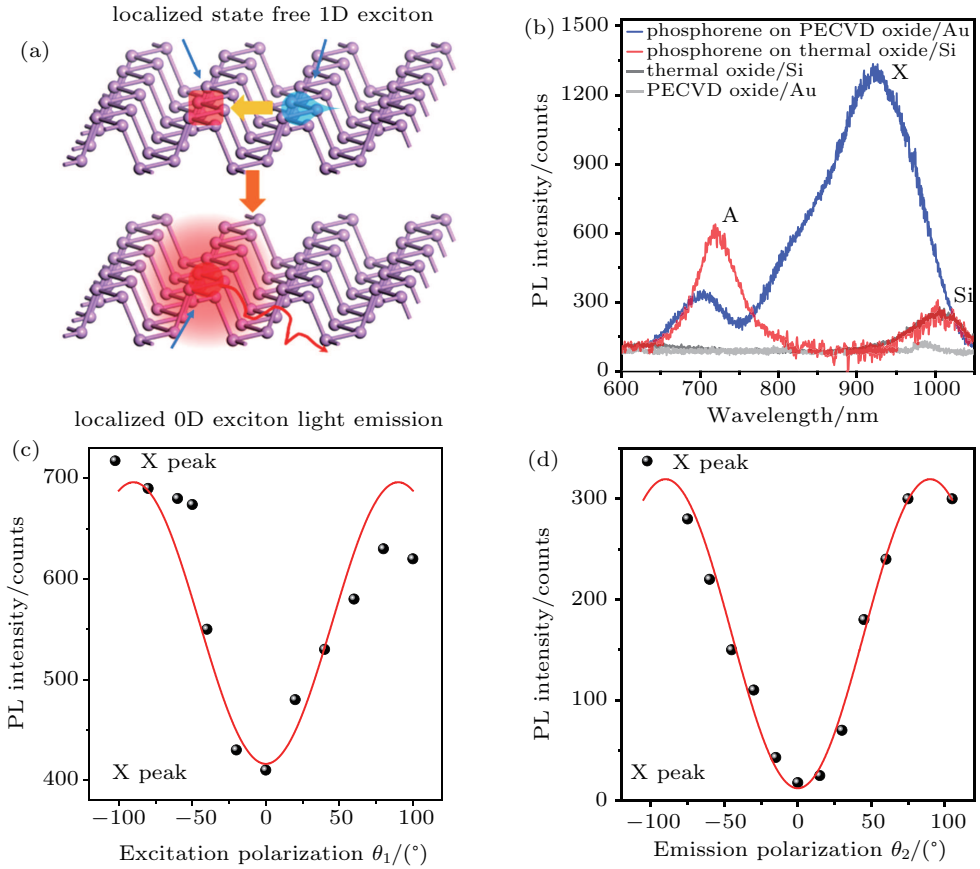


Fig. 6. (color online) Exciton brightening via surface defect engineering on monolayer phosphorene. (a) Schematic plot of free and localized excitons. (b) PL spectra of monolayer phosphorene on thermal oxide and PECVD oxide. (c) Excitation polarization PL results of localized exciton PL peak. (d) Emission polarization PL results of localized exciton PL peak. Figure reproduced from Ref. [49].

5. Conclusion and prospects

We have focused on the optical properties of phosphorene by summarizing our recent work and comparing them with other published papers. Through Raman and polarized PL spectroscopy, the highly anisotropic nature of phosphorene is revealed. Photoluminescence measurements verify the layers-dependent direct bandgap of phosphorene. Furthermore, by applying an electric field or changing the optical injection to the phosphorene system, exciton and trion emissions can be tuned and their dynamics are investigated. The exciton and

trion binding energies are measured to be around one order of magnitude higher than those of TMDs and two orders higher than those of quasi-2D quantum well systems, providing great opportunities for light emitting and energy harvesting applications. We have also discussed the bottleneck of phosphorene applications, that is, the fast degradation of phosphorene in the presence of light and moisture. Several effective encapsulation methods have been introduced, and controllable oxidation of phosphorene has been achieved. By making use of the phosphorus layer and oxygen defects on top of it, new PL emission lines can be generated. The heterostructure of phosphorus oxide and phosphorene even provides abundant opportunities for future optoelectronic applications of phosphorene.

Phosphorene has been demonstrated for various optical and optoelectronic applications due to its unique properties. Photoelectrical conversion is generally considered to be the basis of optoelectronic applications. Lu *et al.* and Wu *et al.* have investigated the photocurrent generation of phosphorene and its oxide in a transistor structure.[54,55] Photodetectors with high responsivity in the near infrared range have been fabricated recently.[56–58] When integrated with a waveguide, photodetectors based on phosphorene exhibit significant advantages over graphene-based ones in their very low dark current.[56] All these applications are limited by the fast degradation of few-layer phosphorene, so suitable encapsulation of phosphorene is essential for its applications. Several methods have proved to be effective, such as using Al_2O_3, PMMA, and hBN to coat the phosphorene sample. *In situ* oxidation of phosphorene top layers to form phosphorus oxide can also work to protect the underlying few-layer phosphorene. Due to its large surface–to-volume ratio and anisotropic nature, phosphorene will be more easily tuned by external media, such as electric bias, magnetic field, and strain. All these tunabilities deserve further exploration.

References

[1] Novoselov K S, Geim A K, Morozov S V, Jiang D, Katsnelson M I, Grigorieva I V, Dubonos S V and Firsov A A 2005 *Nature* **438** 197

[2] Geim A K and Novoselov K S 2007 *Nat. Mater.* **6** 183

[3] Radisavljevic B, Radenovic A, Brivio J, Giacometti V and Kis A 2011 *Nat. Nanotechnol.* **6** 147

[4] Li L, Yu Y, Ye G J, Ge Q, Ou X, Wu H, Feng D, Chen X H and Zhang Y 2014 *Nat. Nanotechnol.* **9** 372

[5] Lee C, Li Q, Kalb W, Liu X Z, Berger H, Carpick R W and Hone J 2010 *Science* **328** 76

[6] Yang J, Wang Z, Wang F, Xu R, Tao J, Zhang S, Qin Q, Luther-Davies B, Jagadish C, Yu Z and Lu Y 2016 *Light Sci. Appl.* **5** e16046

[7] Pei J, Yang J, Xu R, Zeng Y H, Myint Y W, Zhang S, Zheng J C, Qin Q, Wang X, Jiang W and Lu Y 2015 *Small* **11** 6384

[8] Chen H, Yang J, Rusak E, Straubel J, Guo R, Myint Y W, Pei J , Decker M, Staude I, Rockstuhl C, Lu Y, Kivshar Y S and Neshev D 2011 *Sci. Rep.* **6** 22296

[9] Yi Z, Jiong Y, Shuang Z, Salman M, Jiajie P, Xinghua W and Yuerui L 2016 *Nanotechnology* **27** 135706

[10] Lu J, Yang J, Carvalho A, Liu H, Lu Y and Sow C H 2016 *Acc. Chem. Res.* **49** 1806

[11] Pei J, Yang J and L L 2017 *IEEE J. Sel. Top. Quantum Electron.* **23** p. 1

[12] Qiao J, Kong X, Hu Z X, Yang F and Ji W 2014 *Nat. Commun.* **5** 4475

[13] Xia F, Wang H and Jia Y 2014 *Nat. Commun.* **5** 4458

[14] Wang X, Jones A M, Seyler K L, Tran V, Jia Y, Zhao H, Wang H, Yang L, Xu X and Xia F 2015 *Nat. Nanotechnol.* **10** 517

[15] Zhang S, Yang J, Xu R, Wang F, Li W, Ghufran M, Zhang Y W, Yu Z, Zhang G, Qin Q and Lu Y 2014 *ACS Nano* **8** 9590

[16] Mak K F, Lee C, Hone J, Shan J and Heinz T F 2010 *Phys. Rev. Lett.* **105** 136805

[17] Yang J, Lü T, Myint Y W, Pei J, Macdonald D, Zheng J C and Lu Y 2015 *ACS Nano* **9** 6603

[18] Ross J S, Wu S, Yu H, Ghimire N J, Jones A M, Aivazian G, Yan J, Mandrus D G, Xiao D, Yao W and Xu X 2013 *Nat. Commun.* **4** 1474

[19] Liang L, Wang J, Lin W, Sumpter B G, Meunier V and Pan M 2014 *Nano Lett.* **14** 6400

[20] Yang J, Xu R, Pei J, Myint Y W, Wang F, Wang Z, Zhang S, Yu Z and Lu Y 2015 *Light Sci. Appl.* **4** e312

[21] Li L, Kim J, Jin C, Ye G, Qiu D Y, da Jornada F H, Shi Z, Chen L, Zhang Z, Yang F, Watanabe K, Taniguchi T, Ren W, Louie S G, Chen X, Zhang Y and Wang F 2016 arXiv:1601.03103

[22] Koenig S P, Doganov R A, Schmidt H, Castro Neto A H and Özyilmaz B 2014 *Appl. Phys. Lett.* **104** 103106

[23] Buscema M, Groenendijk D J, Blanter S I, Steele G A, van der Zant H S J and Castellanos-Gomez A 2014 *Nano Lett.* **14** 3347

[24] Das S, Zhang W, Demarteau M, Hoffmann A, Dubey M and Roelofs A 2014 *Nano Lett.* **14** 5733

[25] Buscema M, Groenendijk D J, Steele G A, van der Zant H S J and Castellanos-Gomez A 2014 *Nat. Commun.* **5** 4651

[26] Xu R, Yang J, Zhu Y, Yan H, Pei J, Myint Y W, Zhang S and Lu Y 2016 *Nanoscale* **8** 129

[27] Kheng K, Cox R T, d'Aubigné M Y, Bassani F, Saminadayar K and Tatarenko S 1993 *Phys. Rev. Lett.* **71** 1752

[28] Xu R, Zhang S, Wang F, Yang J, Wang Z, Pei J, Myint Y W, Xing B, Yu Z, Fu L, Qin Q and Lu Y 2016 *ACS Nano* **10** 2046

[29] Huard V, Cox R T, Saminadayar K, Arnoult A and Tatarenko S 2000 *Phys. Rev. Lett.* **84** 187

[30] Mak K F, He K, Lee C, Lee G H, Hone J, Heinz T F and Shan J 2013 *Nat. Mater.* **12** 207

[31] Favron A, Gaufres E, Fossard F, Phaneuf-Lheureux A L, Tang N Y W, Levesque P L, Loiseau A, Leonelli R, Francoeur S and Martel R 2015 *Nat. Mater.* **14** 826

[32] Andres C G, Leonardo V, Elsa P, Joshua O I, Narasimha-Acharya K L, Sofya I B, Dirk J G, Michele B, Gary A S, Alvarez J V, Henny W Z, Palacios J J and Herre S J V D Z 2014 *2D Mater.* **1** 025001

[33] Pei J, Gai X, Yang J, Wang X, Yu Z, Choi D Y, Luther-Davies B and Lu Y 2016 *Nat. Commun.* **7** 10450

[34] Zhang G, Chaves A, Huang S, Song C, Low T and Yan H 2016 arXiv:1607.08049

[35] Keyes R W 1953 *Phys. Rev.* **92** 580

[36] Jones A M, Yu H, Ghimire N J, Wu S, Aivazian G, Ross J S, Zhao B, Yan J, Mandrus D G, Xiao D, Yao W and Xu X 2013 *Nat. Nanotechnol.* **8** 634

[37] Plechinger G, Nagler P, Kraus J, Paradiso N, Strunk C, Schüller C and Korn T 2015 *Phys. Status Solidi Rapid Res. Lett.* **9** 457

[38] Tran V, Soklaski R, Liang Y and Yang L 2014 *Phys. Rev. B* **89** 235319

[39] Wood J D, Wells S A, Jariwala D, Chen K S, Cho E, Sangwan V K, Liu X, Lauhon L J, Marks T J and Hersam M C 2014 *Nano Lett.* **14** 6964

[40] Liu H, Du Y, Deng Y and Ye P D 2015 *Chem. Soc. Rev.* **44** 2732

[41] Ziletti A, Carvalho A, Campbell D K, Coker D F and Castro Neto A H 2015 *Phys. Rev. Lett.* **114** 046801

[42] Joshua O I, Gary A S, Herre S J V D Z and Andres C G 2015 *2D Mater.* **2** 011002

[43] Na J, Lee Y T, Lim J A, Hwang D K, Kim G T, Choi W K and Song Y W 2014 *ACS Nano* **8** 11753

[44] Kim J S, Liu Y, Zhu W, Kim S, Wu D, Tao L, Dodabalapur A, Lai K and Akinwande D 2015 *Sci. Rep.* **5** 8989

[45] Cao Y, Mishchenko A, Yu G L, Khestanova E, Rooney A P, Prestat E, Kretinin A V, Blake P, Shalom M B, Woods C, Chapman J, Balakrishnan G, Grigorieva I V, Novoselov K S, Piot B A, Potemski M, Watanabe K, Taniguchi T, Haigh S J, Geim A K and Gorbachev R V 2015 *Nano Lett.* **15** 4914

[46] Avsar A, Vera-Marun I J, Tan J Y, Watanabe K, Taniguchi T, Castro Neto A H and Özyilmaz B 2015 *ACS Nano* **9** 4138

[47] Chen X, Wu Y, Wu Z, Han Y, Xu S, Wang L, Ye W, Han T, He Y, Cai Y and Wang N 2015 *Nat. Commun.* **6** 7315

[48] Li L, Yang F, Ye G J, Zhang Z, Zhu Z, Lou W, Zhou X, Li L, Watanabe K, Taniguchi T, Chang K, Wang Y, Chen X H and Zhang Y 2016 *Nat. Nanotechnol.* **11** 593

[49] Xu R, Yang J, Myint Y W, Pei J, Yan H, Wang F and Lu Y 2016 *Adv. Mater.* **28** 3493

[50] Miyauchi Y, Iwamura M, Mouri S, Kawazoe T, Ohtsu M and Matsuda K 2013 *Nat. Photon.* **7** 715

[51] Ziletti A, Carvalho A, Trevisanutto P E, Campbell D K, Coker D F and Castro Neto A H 2015 *Phys. Rev. B* **91** 085407

[52] Lu J, Wu J, Carvalho A, Ziletti A, Liu H, Tan J, Chen Y, Castro Neto A H, Özyilmaz B and Sow C H 2015 *ACS Nano* **9** 10411

[53] Edmonds M T, Tadich A, Carvalho A, Ziletti A, O'Donnell K M, Koenig S P, Coker D F, Özyilmaz B, Neto A H C and Fuhrer M S 2015 *ACS Appl. Mater. Inter.* **7** 14557

[54] Lu J, Carvalho A, Wu J, Liu H, Tok E S, Neto A H C, Özyilmaz B and Sow C H 2016 *Adv. Mater.* **28** 4090

[55] Wu J, Koon G K W, Xiang D, Han C, Toh C T, Kulkarni E S, Verzhbitskiy I, Carvalho A, Rodin A S, Koenig S P, Eda G, Chen W, Neto A H C and Özyilmaz B 2015 *ACS Nano* **9** 8070

[56] Youngblood N, Chen C, Koester S J and Li M 2015 *Nat. Photon.*

[57] Yu, Zhang S, Zeng H and Wang Q J 2016 *Nano Energy* **25** 34

[58] Engel M, Steiner M and Avouris P 2014 *Nano Lett.* **14** 6414